Mutually injecting semiconductor lasers: simulations for short and zero delay

Nikolay Korneyev [a], Mindaugas Radžiūnas [b], Hans-Jürgen Wünsche[a] and Fritz Henneberger[a]

[a] Humboldt-Universität zu Berlin, Institut für Physik, Newtonstr. 15, 12489 Berlin, Germany

[b] Weierstraß-Institut für Angewandte Analysis und Stochastik, Mohrenstr. 39, 10117 Berlin, Germany

ABSTRACT

Distant lasers with mutual optical injection are subject to a delayed coupling. We consider the barely investigated case of delays shorter than the relaxation oscillation period. In order to illuminate the role of these short delays, the ultimate zero-delay limit is considered as a reference. We use a traveling wave equation model, which fully resolves the spatio-temporal distributions of optical fields and carriers in the lasers and treats the wave propagation between the lasers by delayed boundary conditions. Wavelength detuning between the otherwise identical single-mode DFB lasers is used as primary bifurcation parameter. The zero-delay reference exhibits a synchronisation scenario typical for coupled oscillators. The nonsynchronised regimes represents a self-pulsation of the nonlinear carrier-photon system. Additional effects appear when including a short delay. Resonances of the cavity formed by the laser pair cause a staircase dependence on detuning of the pulsation frequency. Irregular dynamics is observed at the borders of the locked regions as well as at the edges of the stairs.

Keywords: coupled semiconductor lasers, numerical simulation, self-pulsation, synchronisation , delay-coupled oscillator

1. INTRODUCTION

Coupled nonlinear oscillators are a fundamental concept useful in a wide range of sciences. In recent years the influence of a time delay in the coupling of oscillators has become a focus of interest. [1–4] In real system such a delay can occure, e.g., due to spatial separation between the subsystems and a finite propagating time of the coupling signals. The additional degrees of freedom present in such delay-coupled systems may qualitatively alter their dynamical behaviour. On one hand the delayed coupling can result in instabilities and even chaos of formerly stable systems. On the other hand, this delay can be a stabilizing factor of the coupled oscillator systems. Semiconductor lasers (SLs) are ideal candidates for the study of delay-coupled nonlinear oscillators. In this paper we investigate the dynamics of two SLs interacting as sketched in Figure 1. The system consists of two lasers coupled by mutual injection of a certain fraction of the radiation emitted from each laser into the other one.

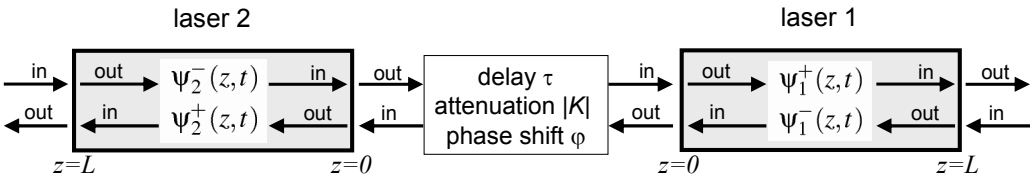

Figure 1. *Scheme of two mutually injecting lasers. To account for symmetry, opposite orientations of the z-axis' within the lasers are used. $z = 0$ and $z = L$ represent the two inner facets and the two outer facets of the laser couple, respectively. With "in" and "out" we label the incoming and outgoing waves at each facet as used in the boundary conditions (6).*

H.J.Wünsche is also with Fraunhofer-Institut Nachrichtentechnik Heinrich-Hertz-Institut, Einsteinufer 37, 10587 Berlin, Germany

The considered type of coupling is characterized by the single pass delay time τ and a complex coupling factor $K = |K|e^{i\varphi}$. The coupling strength is given here by the fraction $|K|$ of the emitted optical amplitude injected into the opposite laser. The phase $\varphi = \omega_0\tau$ represents the optical phase shift along the interconnection at a reference frequency ω_0. Another important parameter in our studies is the detuning $\Delta\omega = \omega_2 - \omega_1$ between the frequencies ω_1 and ω_2 of the uncoupled lasers. All these parameters, in general, are accessible in experiment. The focus of the present paper is to consider the nonlinear dynamics resulting from the interplay of a finite delay time τ and a finite detuning $\Delta\omega$.

The two lasers are supposed to be single mode DFB lasers as used in experimental studies of such configurations. [5] The dynamics of corresponding solitary lasers is well understood: only one attractor is present, which is stationary CW emission at a single wavelength. Upon a perturbation, this attractor is approached via damped relaxation oscillations. Physically, the relaxation oscillations describe a process in which the energy contained inside the laser cavity is periodically exchanged between the number of photons and number of excess carriers (electron-hole pairs). The period τ_{RO} of the relaxation oscillations represents the characteristic time constant of the individual laser. It is typically in the range of some hundred picoseconds.

Comparing τ_{RO} with the delay time τ, one can distinguish different coupling regimes, where qualitatively different dynamics are expected. Long coupling delay $\tau \gg \tau_{RO}$ has already been shown to give rise to rather complex dynamical scenarios.[3] In the present paper we will consider the case of short coupling delay, when the delay time is comparable to or smaller than the relaxation period.

The outline of the paper is as follows. The traveling-wave model with delayed boundary conditions is introduced in Section 2. The method of evaluating the dynamics of coupled lasers by numerically integrating the traveling-wave model is described in Section 3. Results for the zero-delay limit without and with detuning are given in Sections 4 and 5, respectively. The impact of a finite delay on the detuning characteristics is presented in Section 6. Summarizing conclusions are given in Section 8.

2. MODEL

The dynamics of fields and carriers within each DFB laser is described by the Traveling Wave (TW) model. The optical amplitudes $E^{\pm}(z,t)$ of the forward and backward traveling waves are decomposed into slow and fast varying parts according to

$$E_k^{\pm}(z,t) = \psi_k^{\pm}(z,t)\exp\left(i\omega_0 t - i\frac{\pi}{\Lambda}z\right), \qquad (k=1,2). \tag{1}$$

The quantities ω_0: central optical frequency, and Λ: geometrical grating period of the DFB lasers, play a role only as reference for the slowly varying amplitudes which obey the TW equations

$$\frac{\partial}{\partial t}\psi_k^{\pm} = \left[\mp v_g\frac{\partial}{\partial z} + (G_k + i\alpha G_k^o) + i\delta_k - \gamma\right]\psi_k^{\pm} - iv_g\kappa\psi_k^{\mp}. \tag{2}$$

v_g - group velocity, α - line-width enhancement factor, $\gamma = v_g\alpha_0$ - internal optical losses, α_0 -internal absorption, κ - feedback rates of the Bragg gratings. We consider gratings with complex coupling, $\kappa = \kappa' + i\kappa''$, in order to guarantee strict single mode operation. Here, κ' and κ'' are the index and loss contributions, respectively, to the grating strength.

The quantities $\delta_k = \bar{\delta} + (-1)^k\Delta\omega/2$ represent the detuning between the Bragg frequencies (centers of stop bands) and the optical reference frequency ω_0 in case of gain transparency, $G_k^0 = 0$. Their difference is just the detuning $\Delta\omega = \omega_2 - \omega_1$ between the uncoupled lasers, which will be treated as a variable bifurcation parameter. Such a detuning can be obtained in experiments by operating the two lasers at different temperatures. The mean value $\bar{\delta}$ is used to set the frequency center $(\omega_1 + \omega_2)/2$ close to the reference frequency ω_0.

The gain function is depending on carrier and photon densities N_k and S_k,

$$G_k(N_k,S_k) = \frac{G_k^o(N_k)}{1+\varepsilon S_k}, \qquad G_k^o = v_g g'(N_k - N_{tr}), \tag{3}$$

with the differential gain g', the gain compression factor ε (both including the transverse confinement factor), carrier density at transparency N_{tr}. Note that the carrier induced index change $\alpha G_k^o(N_k)$ in Eq. (2) does not contain a nonlinear

Table 1: Parameter values

notation	descibtion	value	unit
$\|K\|^2$	mutual coupling strength	0.05	
κ'	index grating strength	130	cm^{-1}
κ''	loss grating strength	5	cm^{-1}
α_0	internal absorption	25	cm^{-1}
L	Length of lasers	300	μm
c/v_g	group velocity index	3.5	
r	facet reflectivity coefficient	$\sqrt{0.3}$	
ε	nonlinear gain compression factor	10	$10^{-24}m^3$
g'	differential gain	5	$10^{-21}m^2$
I_k	Injection current for both lasers	50	mA
N_{tr}	carrier density at transparency	1	$10^{24}\ \mathrm{m}^{-3}$
τ_n	linear carrier lifetime	$10/3$	ns
V	volume of active zone	5.1	$10^{-17}m^3$
α_H	Linewidth enhancement (Henry) factor	-2	

saturation factor. This choice differs from former application of the TW model [6] having used equal saturation of gain and index. Since nonlinear index saturation has been found to be much smaller than gain saturation, [7,8] its complete neglection seems to be a more reasonable approximation.

The spatially section-wise averaged carrier density N_k is a solution of the rate equation

$$\frac{dN_k}{dt} = \frac{I_k}{eV_k} - \frac{N_k}{\tau_n} - 2G_kS_k. \quad (k=1,2) \tag{4}$$

I_k: injection current, V_k: volume of active zone, e: elementary charge, τ_n: linear carrier lifetime. Supposing proper nomalisation of the optical fields, the average photon densities S_k appearing here can be expressed as

$$S_k = \int_k dz(|\psi_k^+|^2 + |\psi_k^-|^2) \tag{5}$$

in terms of the slowly varying optical amplitudes.

The coupling conditions of the two lasers enter the theoretical description via boundary conditions for the TW Eq. (2). In general, the incoming and outgoing fields at every loss-free laser facet (see Fig. 1) are locally and instantaneously connected by reflection–transmission conditions:

$$\begin{pmatrix}\psi^+\\ \psi^-\end{pmatrix}_{out} = \begin{pmatrix}\sqrt{1-|r|^2} & -r^*\\ r & \sqrt{1-|r|^2}\end{pmatrix}\begin{pmatrix}\psi^+\\ \psi^-\end{pmatrix}_{in}. \tag{6}$$

They contain one complex parameter r, which represents the reflectivity coefficient according to $\psi^-_{out} = r\psi^+_{in}$ in case of $\psi^-_{in} = 0$. The phase of r depends on the position of the facet relative to the Bragg grating. The other coefficients of the matrix follow from amplitude matching and energy conservation. The incoming fields into the lasers at the inner facets $z = 0$ are τ-delayed and K-scaled copies of the output from the inner facets of the opposite lasers. For the outer facets the fields incoming into the lasers are zero:

$$\begin{aligned}\psi^-_{k,in}(L,t) &= 0, && (k=1,2)\\ \psi^+_{k,in}(0,t) &= K\psi^-_{l,out}(0,t-\tau) && (l=3-k,k=1,2)\end{aligned} \tag{7}$$

All parameter values but τ and $\Delta\omega$, which will be varied, are collected in Table 1.

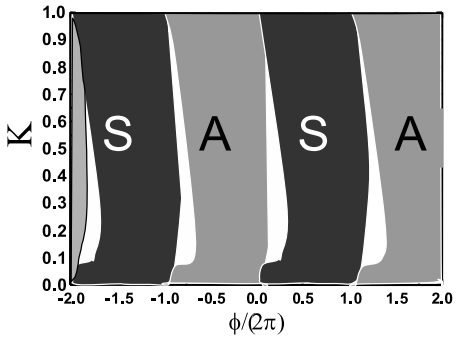

Figure 2. *Regions of completely symmetrical (S) and completely assymmetrical (A) solutions for zero delay and zero detuning. In both regions we observe completely synchronized CW emission. Nonstationary output without these symmetries is obtained in the white regions.*

3. METHOD OF EVALUATING THE DYNAMICS

In order to study the dynamical behaviour of the coupled laser system we solve the Traveling Wave model equations (2-7) numerically. For a given point of operation we integrate them in time domain until the transient stabilizes. Then we continue the calculation for another 10 ns and record the following quantities for a first characterisation of the achieved attractor: minima and maxima of output power at each inner DFB facet, dominant wavelength (position of the highest peak in the optical spectrum from the fast Fourier transform of the outgoing field at each inner DFB facet), and pulsation frequency (the position of the highest peak in the power spectrum from the fast Fourier transform of the power). All these quantities can also be measured with real devices. In addition we also record maximum, minimum, and mean value of the carrier density in each laser. These last quantities are not directly measurable and provide an important insight into the dynamics of the lasers.

To get an overview, we have varied the coupling parameters $|K|, \varphi$, andτ as well as the detuning $\Delta\omega$ over reasonable ranges of values. The final field-carrier state of the previous calculation was always used as initial state for the integration with new parameters. The latter procedure allows to detect hysteresis by changing parameters in different directions.

A complete description of all results goes beyond the scope of a single paper. Here we focus on the dependence on detuning $\Delta\omega$ for two different characteristic delays $\tau = 100$ fs and $\tau = 150$ ps. The first delay time is much shorter than all other characteristic times of the system except the oscillation period of the light $\lambda/c \approx 5$ fs. It corresponds to only 20 wavelengths separation between the two lasers and represents the limit of zero delay. The other delay time is comparable to the relaxation oscillation period τ_{RO} and represents the upper border of the regime of short delay. All other parameters are fixed at values given in Table 1. The coupling strength $|K|^2$ of 5 % roughly corresponds to the experimental setup of Wille et. al..[5] All phenomena depend on coupling phase φ. Throughout the paper we shall present results for $\varphi = \pi$, which exhibits the widest regions of mutual synchronisation.

4. ZERO DELAY LIMIT: SYMMETRIES WITHOUT DETUNING

It is useful first to consider a situation with neither delay nor detuning. This particular case of instantaneously coupled identical laser has been externsively studied very recently[9] as a limit of a coupled system of Lang-Kobayashi rate equations. Exploiting the symmetries of this model, it was shown the existence of stable synchronous or antisynchronous CW-solutions, where the carrier densities are equal ($N_1(t) = N_2(t) = \text{const.}$) and the two complex functions $E_1(t)$ and $E_2(t)$ representing the optical fields within both lasers are related by either $E_1(t) = E_2(t)$ or $E_1(t) = -E_2(t)$, respectively, with $|E_k(t)|^2 = \text{const}$. Furthermore, bifurcations to nonstationary solutions were discovered within the $|K|, \varphi$ plane.

The present TW model equations (2) exhibit the same symmetry with respect to interchange of the two identical lasers. Thus, similar invariant manifolds of synchronous and antisynchronous solutions should exist. In order to check the existence of such solutions and their stability, we analised the numerical solutions by calculating the parameter

$$\eta_s \equiv \eta_s(t) = \frac{P_s(t) - P_a(t)}{P_s(t) + P_a(t)} \qquad \text{with } P_{s,a}(t) = \int_0^L \Big[\left|\psi_1^+(z,t) \pm \psi_2^+(z,t)\right|^2 + \left|\psi_1^-(z,t) \pm \psi_2^-(z,t)\right|^2 \Big] dz. \tag{8}$$

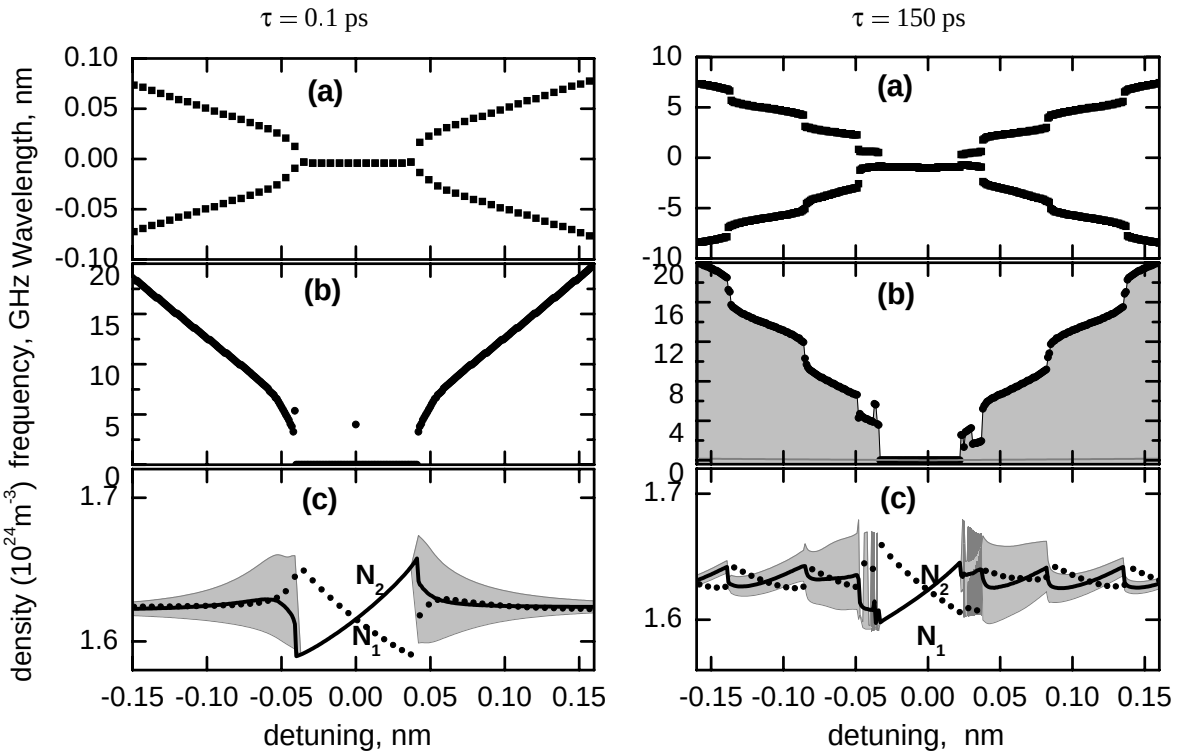

Figure 3. *Characteristics of coupled lasers versus wavelength detuning* $\Delta\lambda = -\Delta\omega\,\lambda_0^2/2\pi c$ *(*$\lambda_0 = 1.54\mu m$*). Left panels: zero delay limit. Right panels: finite delay. Coupling phase* $\varphi = \pi$*. (a): Dominant wavelength of both lasers, (b): main peak position (frequency) of the computed radiofrequency spectra, (c): averages (lines) and all observed positions (shading) of carrier densities in both lasers.*

η_s is between +1 and -1, which limits represent the synchronous and antisynchronous solutions, respectively.

The obtained regions of different symmetries in the $|K|,\varphi$ plane are shown in Fig. 2. Black and grey areas are regions with stable CW synchronous and antisynchronous solutions, respectively. Here we have $N_1 = N_2$ and $\psi_1^{\pm}(z,t) = \psi_2^{\pm}(z,t)$ or $\psi_1^{\pm}(z,t) = \psi_2^{\pm}(z,t)$. Besides these stationary completely synchronized states, we have also found nonstationary states with reduced symmetry in the white portions of Fig. 2. Generally, Fig. 2 is in good agreement with the coresponding figure of Ref.,[9] where the coupled rate equation model was used. Thus, both models do not only have the symmetry but also similar stability properties of the corresponding solutions.

5. DETUNING CHARACTERISTICS: ZERO DELAY LIMIT

Let us consider now the influence of a finite detuning $\Delta\omega \neq 0$ on the coupled lasers, still in the limit of zero delay. The main results of numerically integrating the TW model equations (2-7) are summarized in the left part of Fig. 3. Panels (a), (b) and (c) of this figure show the dominant wavelengths of both lasers, the frequency of the dominant peak in the power spectrum and maximum, minimum and averages of the carrier densities in both lasers, respectively.

Two qualitatively different regimes can be detected within the investigated range of detuning.

At small detunings, the lasers keep in the completely synchronized CW state described in last section for zero detuning. It is characterized by identical wavelengths of both lasers and by the absence of lines at nonzero frequencies in the power spectrum (cf. also upper panels of Fig. 4). Although being locked to each other, the conditions of the oppositely detuned lasers, in general, are slightly different. These differences are represented by the two carrier densities, which within the locked state become identical only at zero detuning (left diagrams of Fig. 3). The asymmetric carrier concentrations also explain the mechanism of wavelength-synchronisation: as long as the detuning is small, the difference between the nominal wavelength of each solitary laser and the identical wavelength of both lasers in the locked state is compensated by the electronic wavelength-shift in connection with the finite α factor.

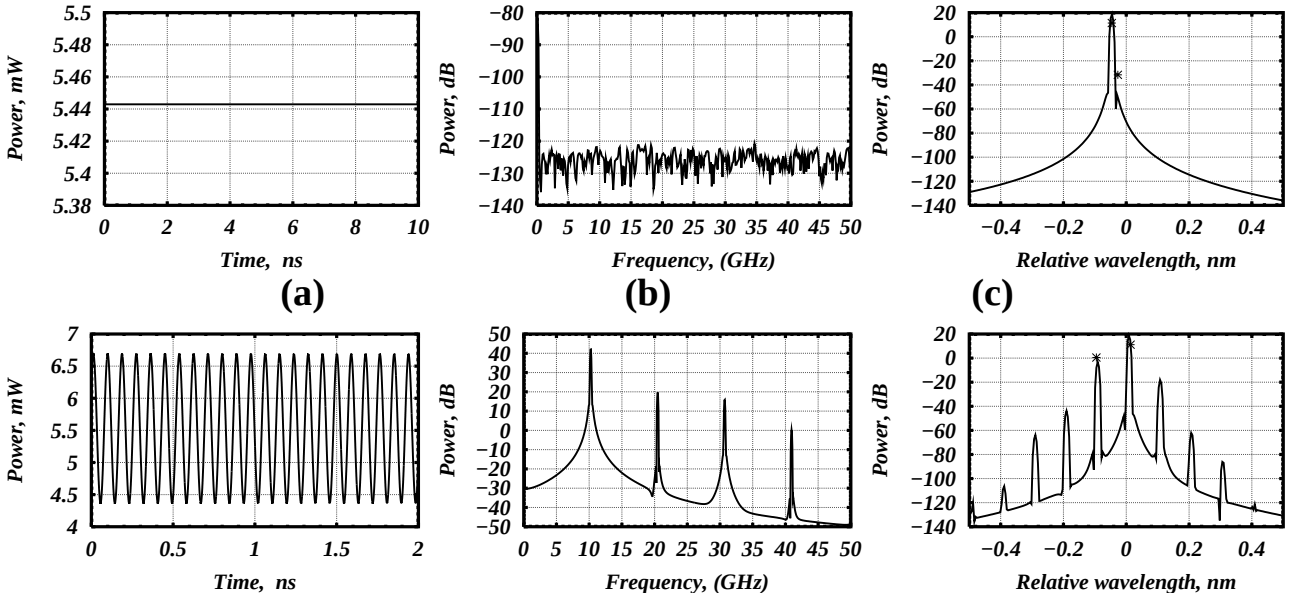

Figure 4.
Synchronisation (upper panels) and beating (lower panels) regimes at zero delay. Typical time trace (a), power (b) and optical (c) spectra at inner facet of Laser 1.

With increasing detuning, the locked state is lost, when the required carrier asymmetry becomes too big. The main wavelengths of the two lasers become different now in connection with a rather sudden readjustment of the carrier densities. In the neighbourhood of the transition, the difference frequency shows a square root like variation which is typical for the synchronisation of periodic oscillations. The extension of the locking interval strictly depends on the coupling phase φ. Here and in the following, we consider only the particular value $\varphi = \pi$. This phase value yielded the largest locking range, while $\varphi = 0$ is corresponding to the smallest one.

In the unlocked regime of operation, Each laser is mainly supporting its own wavelength. However, the optical spectrum of each laser also exhibits a secondary line at the frequency of the opposite laser, due to the finite coupling strength $|K|$. Accordingly, both waves are present in each lasers. Their superposition causes a sinusoidal modulation of the intensity with the difference frequency, which appears as a prominent peak in the power spectra. These beating oscillations of the intensity drive pulsations of the carrier densities, which in turn act back on the intensity. In general, a self-sustained pulsation of the whole nonlinear carrier-photon system is the result. The nonlinear interaction also gives rise to the higher harmonics appearing in the power spectra (lower panel (b) of Fig. 4). In addition, it causes a series of satellites in the optical spectra due to nondegenerate four-wave mixing (lower panel (c) of Fig. 4).

The amplitude of the carrier pulsations is indicated as grey shaded region in Figure 3c. It decreases with increase of the detuning $|\Delta\omega|$. The amplitude of the power oscillation shows a similar behaviour. At sufficiently large detuning, the oscillations become negligible and the two lasers operate like independent devices.

6. DETUNING CHARACTERISTICS: FINITE DELAY

In this section we consider the detuning characteristics in case of a coupling delay $\tau = 150$ ps, which is representative for the upper border of the regime of short delay. The results are summarized in the right panels of Fig. 3.

As in the instantaneous coupling limit, we also find complete synchronisation for small detuning and beating-induced self-pulsations for larger detunings. In the unlocked regime, the oscillation amplitude also decreases with increasing detuning $|\Delta\omega|$.

At the same time, some new prominent features are clearly observed in the unlocked regime. Most striking difference in comparison with zero delay is a discontinuous staircases-like shift of the operating wavelengths and of the according pulsation frequencies with increasing detuning. On every stair, each of the two wavelengths of the coupled lasers shifts distinctly less than those of the uncoupled lasers. This retardation of the wavelength shift appears in combination with asymmetric changes of the carrier densities which are apparently similar to those within the central locking region. The different stairs are interrupted by cyclic sudden jumps of the wavelengths in connection with readjusting carrier densities. The cycles are approximately 0.05 nm wide, which very well corresponds to the round-trip frequency $1/2\tau$. From this point of view, the stairs can be interpreted in terms of locking of the frequency difference between the two lasers to integer multiples of the round trip time. We have observed this phenomenon for a wide range of parameters and regard it as a common feature of mutually interacting lasers in the short delay regime.

In addition to the described beating-induced regular self-pulsations, even more complex irregular dynamics appears at the borders of the central synchronisation region as well as at some edges of the stairs just before the wavelength jumps. The detailed description and analysis of these states is beyond the scope of the present paper.

7. MODE ANALYSIS

In order to better understand the described detuning characteristics in case of a finite delay, we have performed a mode analysis.[12] Although the concept of modes is basic in laser physics, there exist many different versions depending on context. In general, the set of optical modes represents all possible natural oscillations of the optical field in a resonator. The standing waves in a usual Fabry-Perot cavity may serve as a well-known example. In the present context, we consider the modes of the compound cavity formed by the two coupled lasers. In particular, we consider the solutions of TW equations (2) and boundary conditions (6,7) with constant gain values G_k, G_k^0. The latter values are taken from temporal averages of the results of full simulation calculations for the given point of operation. Mode fields vary exponentially with time, $\psi \sim \exp(i\Omega t)$. In general, an infinite number of solutions with different complex mode frequencies Ω exist. Real and imaginary parts of these frequencies represent the modal optical frequencies and and decay rates, respectively.

Figure 5 presents modal wavelengths and decay rates (damping) in the relevant spectral range. They have been accordingly calculated for the same configuration as in the right column of Fig. 3. Two types of modes can be distinghuished: dominant modes whose wavelengths agree with the spectral peaks of the simulation calculation and a comb of side modes in between.

In the central locking range, only one dominant mode exists. All modes but this one are highly damped and do not contribute to the laser emission in this CW regime.

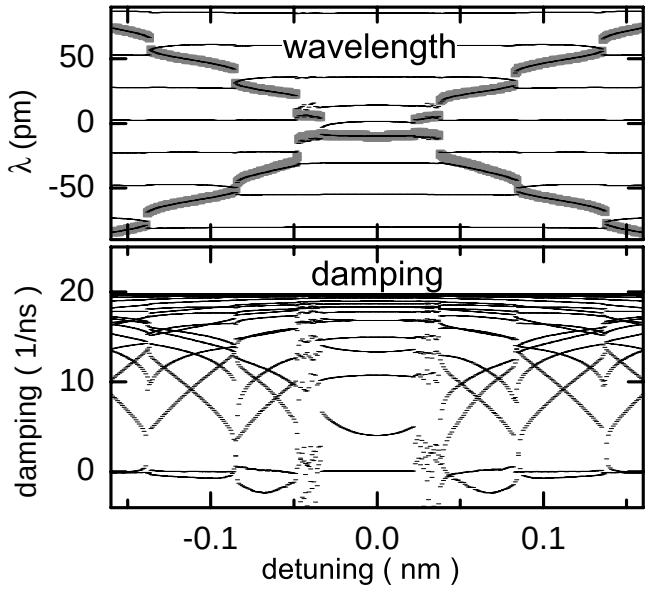

Figure 5. Mode analysis of the simulation calculations of the right column of Fig. 3. Upper penal: wavelengths. Thick grey: simulation calculation. Thin: modes. Lower penal: decay constants of the modes.

Within the unlocked staircase regions, two dominant modes coexist. All other modes are highly damped and play no role. In contrast to the locked regime, the damping of the dominant modes is not exactly zero. This is possible, because the evolution of modal powers is not only determined by their damping constants, but also by mutual feeding of the modes in case of nonstationary carrier densities.[12] With increasing detuning, the amplitude of the carrier oscillations decreases (Fig. 3c) and, hence, the damping of both main modes approaches zero.

The damping of side modes moves down towards zero when its wavelength is crossed by a dominant mode. These crossings determine the edges of the stairs in the wavelength picture. The undamped side mode takes over the lasing here, whereas a formerly dominant mode becomes a side mode. At the border of the locked region, the interaction of at least three undamped modes, which in addition have nearly degenerate wavelengths, causes an irregular behavior (Fig. 3c, right panel). The extension of these ranges with irregular behaviour increases with coupling strength $|K|$.

8. CONCLUSION

Two coupled DFB lasers have been simulated using a traveling wave model. Instantaneous coupling has been compared with a short (150 ps) coupling delay. Both zero and short delay show synchronisation of the lasers at small detuning and, otherwise, two-wavelength operation. The unlocked regime represents a self-pulsation of the nonlinear carrier-photon system, which is driven by the beating between the two waves. Delay causes additional effects, such as a staircase-type frequency-detuning characteristics and irregular dynamics at the stair edges. Mode analysis allows to attribute these effects to the interaction of the lasers with delay-induced cavity resonances.

The work was supported by Deutsche Forschungsgemeinschaft in the framework of Sfb 555.

REFERENCES

1. H.G.Schuster and P.Wagner, ”Mutual entrainment of two limit cycle oscillators with time delayed coupling”, Progress of Theoretical Physics 81, no. 5, 939-945 (1989)
2. S. H. Strogatz, “Death by delay”, *Nature*, 394, (316-317) 1998
3. T.Heil, I.Fischer, W.Elsäßer, “Chaos Synchronization and Spontaneous Symmetry-Breaking in Symmetrically Delay-Coupled Semiconductor Lasers”, *Phys. Rev.Lett.*, 88, 795-798 (2001)
4. F. Rogister and J. Garcia-Ojalvo, “Symmetry breaking and high-frequency periodic oscillations in mutually coupled laser diodes”, *Opt. Lett*, 28, 1176-1178, (2003)
5. E.Wille, M.Peil, I.Fischer, W.Elsäßer “Dynamical scenarious of mutually delay-coupled semiconductor lasers in the short coupling regime”, in “ *proc. of SPIE , Semiconductor Lasers and Laser Dynamics*, Vol.5452 , 27-30 April 2004
6. O. Brox et al., “High-Frequency Pulsations in DFB-Lasers with Amplified Feedback”, *IEEE J. of Quantum Electronics*, Vol. 39, no. 11, pp. 1381- 1387 (2003).
7. M.A. Summerfield and R.S. Tucker, ”Frequency-domain model of multiwave mixing in bulk semiconductor optical amplifiers”, *IEEE J. of Selected Topics in Quantum Electronics*, Vol. 5, no. 3, pp. 839-850 (1999).
8. R. Gutieerrez-Castrejon, L. Schares, L. Occhi, and G. Guekos, ”Modeling and measurement of longitudinal gain dynamics in saturated semiconductor optical amplifiers of different length”, *IEEE J. of Quantum Electronics*, Vol. 36, no. 12, pp. 1476-1488 (2000).
9. S.Yanchuk, K.Schneider, L.Recke “ Dynamics of two mutually coupled semiconductor lasers: instantaneous coupling limit”, in “ *proc. of SPIE , Semiconductor Lasers and Laser Dynamics*, Vol.5452 , 27-30 April 2004
10. J. K. White, M. Matus, and J. V. Moloney “Achronal generalized synchronization in mutually coupled semiconductor lasers”, *Phys. Rev. E*, 65, 036229 (2002).
11. M. Möhrle et al., “Detuned Grating Multisection-RW-DFB Lasers for High Speed Optical Signal Processing”, *IEEE J. Sel. Top. Quantum Electron*. Vol. 7, pp. 217 –223 (2001).
12. M. Radziunas and H.-J. Wünsche, “Multisection semiconductor lasers: àlongitudinal modes and their dynamics”, to appear in *Optoelectronic devices - advanced simulation and analysis* (ed. J. Piprek), Springer New-York, 2004.